molecular pharmaceutics

Article

pubs.acs.org/molecularpharmaceutics

Transformation of Oligomers of Lipidated Peptide Induced by Change in pH

Ying Wang,[†] Aleksey Lomakin,[†] Sonoko Kanai,[‖] Rainer Alex,[‖] and George B. Benedek*[,†,‡,§]

[†]Materials Processing Center, [‡]Department of Physics, and [§]Center for Materials Science and Engineering, Massachusetts Institute of Technology, 77 Massachusetts Avenue, Cambridge, Massachusetts 02139, United States

[‖]Roche Pharmaceutical Research and Early Development, Small Molecule Research, Roche Innovation Center Basel, F. Hoffmann-La Roche Ltd, Grenzacherstrasse 124, 4070 Basel, Switzerland

Supporting Information

ABSTRACT: Oligomerization of lipidated peptides is of general scientific interest and is important in biomedical and pharmaceutical applications. We investigated the solution properties of a lipidated peptide, Liraglutide, which is one of the glucagon-like peptide-1 (GLP-1) agonists used for the treatment of type II diabetes. Liraglutide can serve as a model system for studying biophysical and biochemical properties of micelle-like self-assemblies of the lipidated peptides. Here, we report a transformation induced in Liraglutide oligomers by changing pH in the vicinity of pH 7. This fully reversible transformation is characterized by changes in the size and aggregation number of the oligomer and an associated change in the secondary structure of the constituent peptides. This transformation has quite slow kinetics: the equilibrium is reached in a course of several days. Interestingly, while the transformation is induced by changing pH, its kinetics is essentially independent of the final pH. We interpreted these findings using a model in which desorption of the monomer from the oligomer is the rate-limiting step in the transformation, and we determined the rate constant of the monomer desorption.

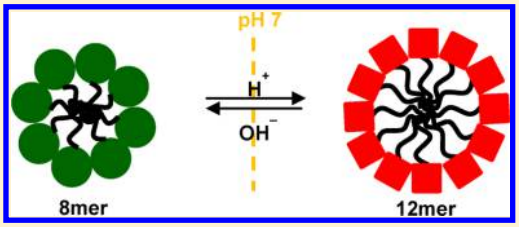

KEYWORDS: *peptide amphiphile, incretin, micelle, oligomerization, self-assembly, light scattering*

INTRODUCTION

Peptides constitute a growing class of biologics developed to treat a variety of diseases, such as cancers, heart disease, and diabetes.[1−3] Many therapeutic peptides are biomimetic drugs, and like their naturally occurring analogues that perform important biochemical functions, they have high potency and high selectivity. However, since the level of such peptides (usually hormones) is tightly regulated in the human body, development of peptide therapeutics often encounters the challenges of short in vivo lifetime and low stability.[1] Human glucagon-like peptide-1 (GLP-1) analogues are an important group of peptide drugs for the treatment of type II diabetes.[4,5] The GLP-1 agonist drugs increase glucose-dependent insulin secretion and inhibit glucagon secretion.[6,7] Despite their excellent ability in controlling blood sugar level, the therapeutic effect of the GLP-1 agonists is greatly limited by fast degradation of these peptides in blood catalyzed by the dipeptidyl peptidase 4 (DPP-4).[4−6] There are two common strategies to extend the circulating lifetime of these peptides: first is to introduce mutations to the DPP-4 cleavage site, i.e., the second and third amino acids at the N-terminal of the peptide; the other method is to link the peptide to conjugates such as albumin, polyethylene glycol (PEG), or fatty acids.[4,5,8]

Lipidation is a common approach to modify bioactive peptides and improve their pharmaceutical properties.[9−14] The lipidated peptides can acquire amphiphilic properties. In vivo, they can bind to serum albumin and form micelle-like assemblies. These characteristics of peptide amphiphiles can improve their structural stability, circulating half-life, cell internalization, and other pharmacokinetic properties.[9−13] Assemblies of the peptide amphiphiles are of particular interest in biophysical and pharmaceutical research.[15−20] These assemblies have micelle-like features. They are in thermodynamic equilibrium with the peptide monomers and have labile structures. The rate constant of monomer desorption from such peptide assemblies is an important parameter that determines stability and pharmacokinetic behavior of bioactive peptides.[15−18] Like regular micelles, the properties of the assemblies of peptide amphiphiles depend on environmental factors such as solution temperature, pH, ionic strength, salts, and other solution components. Conversely, the response of these peptide assemblies to changes in environmental factors can shed light on their stability and dynamic behavior in formulation conditions and in vivo.

Liraglutide, $R^{34}K^{26}$-(*N*-ε-(γ-Glu(*N*-α-oxohexadecanoyl)))-GLP-1[7−37], is a GLP-1 agonist drug that requires only once-a-day administration. Its amino acid sequence is identical to the human GLP-1[7−37] except for the K34R mutation. A palmitic acid is linked through a glutamic acid to the 20th amino acid residue (lysine) of Liraglutide (Supporting Information S-1). The lipid conjugation renders Liraglutide a

Received: July 29, 2014
Revised: December 9, 2014
Accepted: January 8, 2015
Published: January 8, 2015

DOI: 10.1021/mp500519s
Mol. Pharmaceutics 2015, 12, 411−419

long half-life in blood, hypothetically through promoting oligomerization and allowing monomer binding to serum albumin.[8,21,22] Previous studies[21] have indicated that Liraglutide forms stable heptamers in the formulation buffer (10 mM Tris/ClO_4, pH 8.0) and that the oligomerization stabilizes the secondary structure, mainly α helical, of the peptide.

In this work, we used Liraglutide as a model peptide to study the effect of solution conditions on oligomerization of lipidated incretin peptides. In particular, we observed a pH-induced transformation of the micelle-like oligomer of Liraglutide. We found that the Liraglutide octamer (8mer) in sodium phosphate buffer transforms into the dodecamer (12mer) as the pH drops below pH 6.9. The change in the oligomer size is accompanied by a change in the peptide structure. This oligomer transformation is completely reversible when pH increases back above 6.9. Since the pH at which this transformation occurs is likely to depend on the amino acid sequence of the peptide, it could be encountered in medical and biological studies of future incretin peptide drugs. Furthermore, we found that this oligomer transformation is a very slow process and that the transformation rate is insensitive to pH. We argue that the monomer desorption is the rate limiting step in this pH-induced transformation. The rate constant of monomer desorption can be deduced through monitoring the kinetics of the oligomer transformation. Since pH-induced changes of peptide interaction and structure are common phenomena, this work can be useful for developing future drugs and formulations and for understanding biophysical properties of peptide amphiphiles.

MATERIALS AND METHODS

Materials and Solution Preparation. Lyophilized Liraglutide with purity higher than 95% was purchased from CS Bio Co., Menlo Park, CA (Lot # L265). The purity of Liraglutide was tested by reverse phase high performance liquid chromatography (HPLC) with a C8 column. The molecular weight of Liraglutide monomer measured by mass spectrometry is 3751.01 g/mol (the expected value is 3751.20 g/mol). The 10 and 20 mM sodium phosphate buffers were prepared using $NaH_2PO_4{\cdot}H_2O$ and NaH_2PO_4 (Mallinckrodt Chemicals, St. Louis, MO). NaCl (Sigma-Aldrich, St. Louis, MO) was added to prepare the 20 mM phosphate buffer with 0.1 M NaCl. All buffers were filtered through membrane filters with the pore size 0.45 μm (Millipore, Bedford, MA). Liraglutide powder was dissolved in phosphate buffer at pH 8.1 to prepare solutions with given concentrations. The peptide concentration was measured using a UV spectrometer (DU640, Beckman Coulter, Brea, CA). The extinction coefficient of Liraglutide at 280 nm, ε_{280} = 1.99 L/g·cm, was calculated from its amino acid sequence using the ProtParam tool on the ExPASy Bioinformatics Resource Portal (www.expasy.org). The isoelectric point of Liraglutide is 4.0 (reported in the Pharmaceutical Interview Form: Victoza, Japanese version fourth Edition July 2011). The pH of solution was measured using a microelectrode (Orion 9863BN, Thermo Scientific, Waltham, MA) with the accuracy of ±0.02 pH units.

Quasi-Elastic Light Scattering (QLS) Experiments. Since light scattering experiments are very sensitive to high molecular weight aggregates, all samples for the QLS measurements were incubated at pH 8.1 and room temperature for 1 day to disassemble the preexisting aggregates. Before the QLS measurements, the pH of the solution was carefully adjusted to the desired value using small amounts of 1 M phosphoric acid and 1 M sodium hydroxide. One hundred microliters of each sample was filtered through a 22 nm cutoff syringe filter (Whatman) and placed in a test tube. The QLS experiments were performed on a custom-made light-scattering apparatus using a correlator (PD2000 DLS PLUS, Precision Detectors, Bellingham, MA) and a Coherent He−Ne laser (35 mW, 632.8 nm; Coherent Inc., Santa Clara, California). The temperature of the sample compartment was controlled by a water circulator and recorded by a thermocouple. All measurements were performed at a scattering angle of 90°. The measured correlation functions were analyzed by the Precision Deconvolve 5.5 software (Precision Detectors) using a regularization algorithm to calculate the distribution of the apparent diffusion coefficient, D, of the peptide in the solutions. The apparent hydrodynamic radius, R_h, was calculated from D using the Stokes−Einstein equation, $R_h = kT/6\pi\eta D$. The viscosities of the phosphate buffers, η, at the QLS experimental temperatures were determined using a glass capillary viscometer (A223, CANNON). The viscosities of the 20 mM phosphate buffer with/without 0.1 M NaCl at 22.0 °C are, respectively, 1.00 and 1.02 cP.

Static Light Scattering (SLS) Experiments. To determine aggregation number and second virial coefficient of Liraglutide oligomer, we conducted SLS experiments. In a SLS experiment, a series of samples at different peptide concentrations were prepared in the same way as for the QLS measurements. A blank buffer and a HPLC grade toluene (Sigma-Aldrich) were also measured in each SLS experiment for calibration of the instrument. Five microliters of each sample was placed into a cubic quartz cuvette (Micro-CUVETTE, Wyatt Technology, Santa Barbara, CA), and the scattered intensity was measured at a fixed angle of 90° using the DynaPro NanoStar (Wyatt Technology) light scattering instrument with a 633 nm laser. The instrument was set at 22.0 °C and equilibrated before the experiments. The instrument simultaneously collected both SLS (intensity) and QLS (intensity fluctuation) data. The QLS data was analyzed by the Dynamics software (Wyatt Technology) with a regularization algorithm and allowed separation of trace amount of preexisting small aggregates from the main oligomer. The fraction of the light scattered by the aggregates was subtracted from the total intensity. The corrected light intensity, I_S, was used to calculate the excess Rayleigh ratio at 90° for the Liraglutide oligomer, $R_{90°} = R_{90°,r}(n_0^2/n_r^2)(I_s - I_{s,0})/I_{s,r}$. Here, n_0 = 1.333 and n_r = 1.492 are, respectively, the refractive indexes of the buffer and toluene (the standard) at 22 °C. $R_{90°,r} = 1.359 \times 10^{-5}$ cm^{-1} is the Rayleigh ratio of toluene at 22 °C and the scattering angle of 90°.[23] $I_{s,0}$ and $I_{s,r}$ are, respectively, the measured scattering intensities of the buffer and toluene at 22 °C.

From the concentration dependence of the excess Rayleigh ratio, the molecular weight, M, and the second virial coefficient, B_2, were obtained using equation $Kc/R_{90°} = 1/M + 2B_2c$, where c is the mass concentration of the peptide and K is the optical coefficient given by $K = 4\pi^2 n_0^2(dn/dc)^2/(N_A\lambda^4)$. N_A is the Avogadro's number, and λ is the wavelength of the laser in vacuum. The refractive index increment associated with the peptide concentration, dn/dc = 0.182 mL/g, was measured at 22 °C using a refractometer (ABBL-3L, Bausch and Lomb). Accuracy within 5% of the SLS experiments was confirmed by measuring a standard protein, recombinant human eye lens Crystallin gamma D, with known molecular weight.

DOI: 10.1021/mp500519s
Mol. Pharmaceutics 2015, 12, 411−419

Circular Dichroism (CD) Experiments. Samples of ~0.2 mg/mL Liraglutide in 10 mM sodium phosphate buffer were prepared for CD experiments. All samples were filtered through 22 nm syringe filters. The exact concentrations of the samples were measured by UV absorbance. Three hundred microliter aliquots of each sample was placed in a 1 mm pathway far-UV quartz cuvette (NE-1-Q-1, New Era, Vineland, NJ), and the far-UV CD spectra were collected at 22 °C by an Aviv 202 CD spectrometer. The spectra were collected over the wavelength range from 250 to 195 nm with the 1 nm interval, and data at each wavelength was averaged over 30 s. The CD spectrum of the 10 mM phosphate buffer was subtracted from the spectra of the samples. The mean residue ellipticity, θ, was calculated from the measured ellipticity, θ_{obs}, using the relationship $\theta = \theta_{obs}M_0/cln$, where M_0 is the molecular weight of Liraglutide monomer, c is the mass concentration of the peptide, l is the path length of the cuvette, and $n = 32$ is the number of amino acid residues in a Liraglutide molecule.

RESULTS

Oligomerization of Liraglutide at Physiological pH. Liraglutide is a lipid-conjugated peptide that is expected to form oligomers in aqueous solution.[21] In our QLS experiments, we observed that Liraglutide in 20 mM sodium phosphate buffer at pH 7.4 has a narrow size distribution (Figure 1 inset), and the hydrodynamic radius is equal to 2.8 ± 0.1 nm as obtained by extrapolation to infinite dilute solutions (Figure 1). This value is too large for a Liraglutide monomer whose molecular weight is lower than 4 kDa. For a rough comparison, human γD Crystallin, a globular protein with molecular weight 21 kDa, has R_h = 2.3 ± 0.1 nm.[24] Thus, the value of hydrodynamic radius of Liraglutide is consistent with oligomer formation. In the SLS experiment, we have determined that the molecular weight of Liraglutide oligomer in this buffer is 30 ± 2 kDa (Figure S1, Supporting Information). This molecular weight corresponds to an aggregation number m = 8.0 ± 0.4, which is compatible with the value m = 7 previously determined by analytical ultracentrifugation experiments for Liraglutide in a different buffer (10 mM Tris/ClO_4 buffer at pH 8.0).[21] Furthermore, the light scattering experiments show that both hydrodynamic radius and the intensity of scattered light are constant within experiment error over a range of temperatures from 5 to 37 °C (Figure S2, Supporting Information). These results indicate that the 8mer of Liraglutide at pH 7.4 is quite stable, and there is no significant shift of the oligomerization equilibrium within this temperature range.

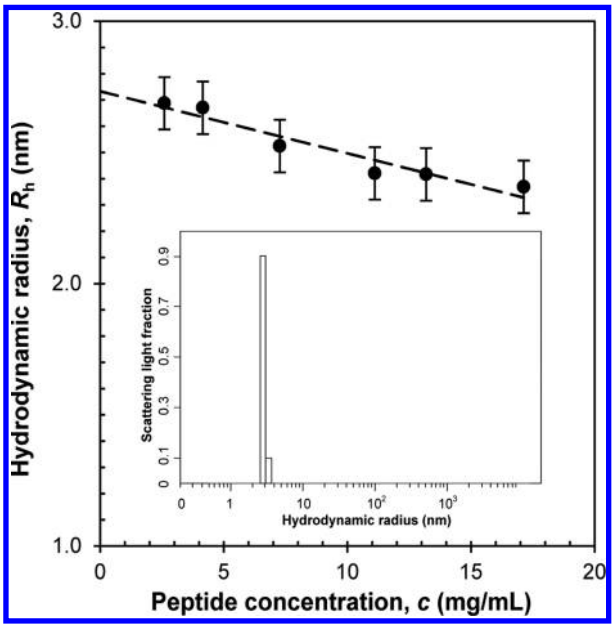

Figure 1. Apparent hydrodynamic radius, R_h, of Liraglutide in 20 mM sodium phosphate buffer at pH 7.4 and 22 °C as a function of the peptide concentration. The inset (c = 17 mg/mL) is a typical histogram of hydrodynamic radius distribution of a Liraglutide sample.

According to Figure 1, the apparent hydrodynamic radius of Liraglutide slightly decreases as the peptide concentration increases. The negative slope of dR_h/dc implies a repulsive interaction between the Liraglutide oligomers. The positive value of the second virial coefficient determined from the SLS data, B_2 = (1.2 ± 0.2) × 10^{-6} mol·L/g^2, also indicates interoligomer repulsion. Considering the acidic isoelectric point of Liraglutide (pI = 4.0), the interoligomer repulsion could be attributed to the electrostatic interaction between the negative charges on the peptides at pH 7.4. Clearly, the repulsive interaction plays an important role in maintaining the solubility of Liraglutide at physiological pH.

pH-Dependence of the Size of Liraglutide Oligomer. The solution pH determines the charges of the amino acid residues and consequently affects the oligomeric state of Liraglutide and the interoligomer interactions. We have examined the pH effect by QLS and SLS experiments. The samples were prepared in 20 mM phosphate buffer at pH 8.1, and the pH was adjusted to the desired values using concentrated phosphoric acid or sodium hydroxide.

Below pH 6.3, aggregation of Liraglutide was detected within 10 min (Figure S3A, Supporting Information), and over time, amorphous aggregates can be observed under a light microscope (Figure S3B, Supporting Information). Aggregation of Liraglutide at low pH is expected since the net charge on the peptide as well as the electrostatic repulsion decreases as pH approaches the isoelectric point.

At pH above 6.3, Liraglutide is soluble, and the QLS experiments show no formation of large aggregates for at least 2 weeks. In Figure 2, we present the pH dependence of the apparent hydrodynamic radius, R_h, of Liraglutide oligomer in the pH range from 6.4 to 9.2. In this figure, the apparent hydrodynamic radius, R_h, varies with the peptide concentration. As we have discussed in the previous section, the concentration dependence of R_h is due to the repulsive interoligomer interaction, which results in an increase of diffusion coefficient as the peptide concentration increases. The hydrodynamic radius of the oligomer in the absence of interoligomer interaction is estimated by extrapolating R_h to zero peptide concentration (see Figure 1). Above pH 6.9, R_h of Liraglutide oligomer is essentially independent of pH and the extrapolated hydrodynamic radius is R_{h1} = 2.8 nm. In the pH range from 6.3 to 6.9, Figure 2 shows a sharp increase in R_h as the pH decreases. At pH 6.4, the lowest pH at which no aggregation occurs, the hydrodynamic radius extrapolated to zero peptide concentration is R_{h2} = 3.3 nm.

We calculated the aggregation numbers of Liraglutide oligomers at different pHs using the results of SLS experiments (Figures 1S and 4S, Supporting Information). The aggregation number of the oligomer increases from m_1 = 8.0 ± 0.4 at pH 7.4 to m_2 = 12.0 ± 0.6 at pH 6.4 and pH 6.7. This 50% increase of the aggregation number is consistent with the increase of

DOI: 10.1021/mp500519s
Mol. Pharmaceutics 2015, 12, 411−419

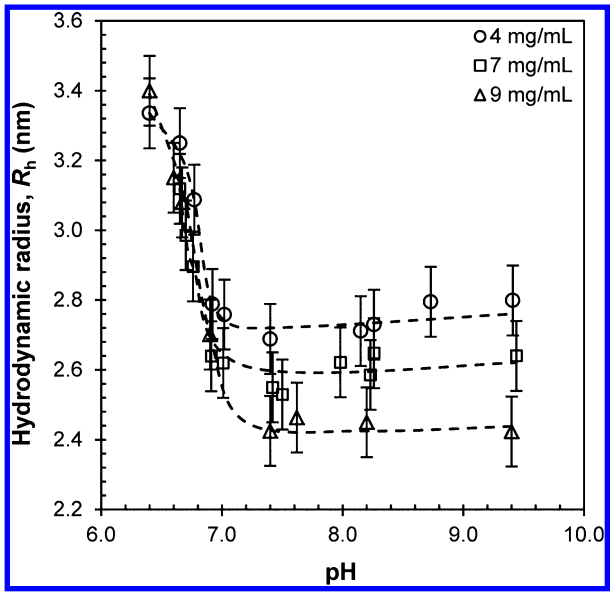

Figure 2. Apparent hydrodynamic radius, R_h, of Liraglutide as a function of pH from pH 6.4 to pH 9.4 measured by QLS at 22 °C. At all three concentrations, R_h increases markedly at pH below pH 6.9. The dashed curves are the eye guides for the data.

hydrodynamic radius measured by QLS, $(R_{h2}/R_{h1})^3 \approx 1.5$. The SLS experiments also yield the second virial coefficients at pH 6.4 and pH 6.7, respectively: $B_2 = (2.0 \pm 0.5) \times 10^{-7}$ and $(5.0 \pm 0.5) \times 10^{-7}$ mol·L/g^2, which are significantly smaller than that at pH 7.4. This result is consistent with the decrease of the electrostatic repulsion between oligomers upon lowering pH.

In Figure 3, we show a similar pH dependence of the size of Liraglutide oligomer at ionic strength close to physiological value, in 20 mM phosphate buffer with 0.1 M NaCl. At the peptide concentration 4 mg/mL, the apparent hydrodynamic radius of Liraglutide at high ionic strength is noticeably larger

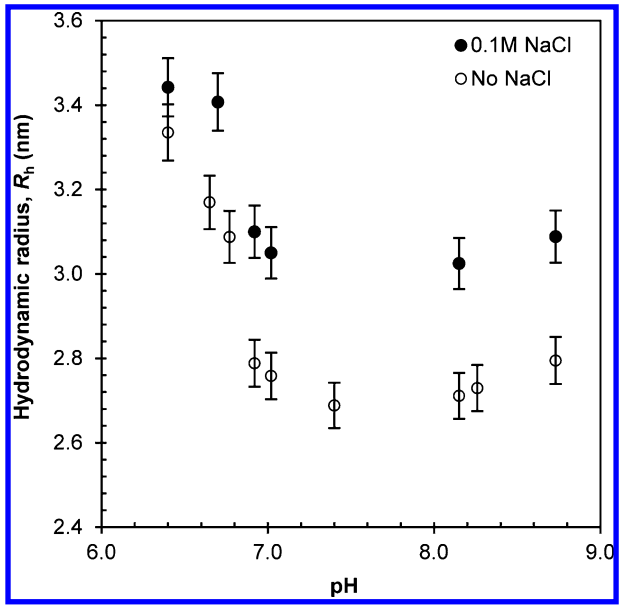

Figure 3. Apparent hydrodynamic radius, R_h, of Liraglutide as a function of pH at peptide concentration 4 mg/mL in 20 mM sodium phosphate buffer with 0 M (open circles) and 0.1 M NaCl (solid circules) measured by QLS at 22 °C. R_h increases markedly at pH below pH 6.9.

than that at the low ionic strength. This observation reflects a much weaker concentration dependence of the apparent hydrodynamic radius at high ionic strength than that shown in Figure 1. The weak concentration dependence of R_h at high ionic strength is due to reduction of repulsive interoligomer interaction by the electrostatic screening effect.

Kinetics of the pH-Induced Transformation of Liraglutide Oligomer. The protonation of amino acids in aqueous solutions is expected to occur in microseconds.[25] However, we found that the kinetics of the pH-induced transformation of Liraglutide oligomer is quite slow. Figure 4A

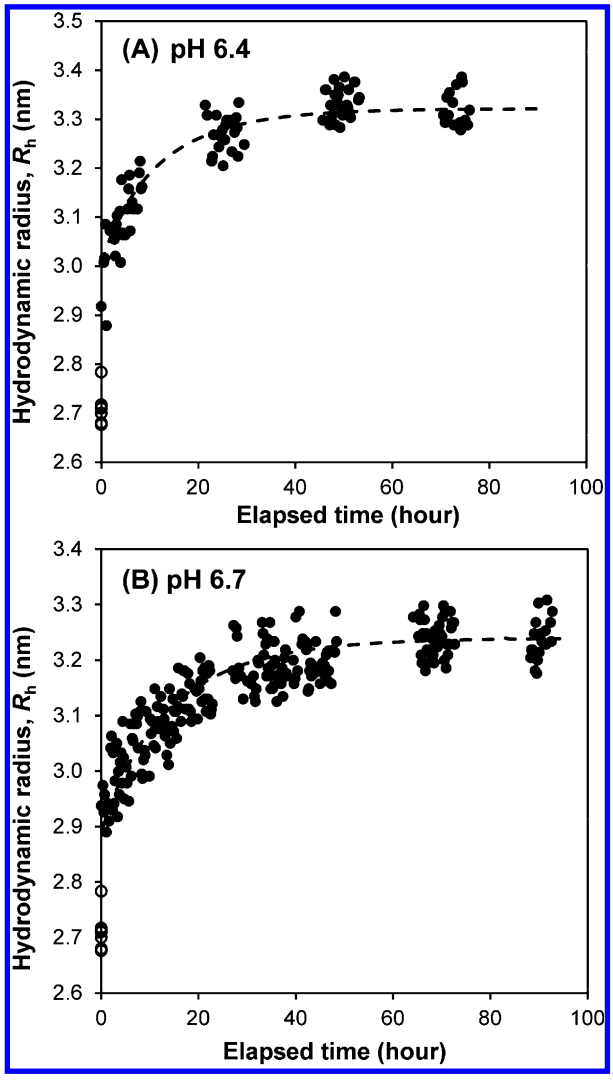

Figure 4. After the pH was lowered from 8.1 to (A) 6.4 and (B) 6.7, the hydrodynamic radius, R_h, of Liraglutide in a 4 mg/mL solution as a function of time was monitored by QLS at 22 °C. The open circles represent the R_h of Liraglutide in the initial solutions at pH 8.1. The solid circles represent the R_h of Liraglutide in the solutions at pH 6.4 and pH 6.7. The dashed curves are the fits of the data with first order rate law as described in the discussion section.

shows that, after lowering pH from 8.1 to 6.4, the hydrodynamic radius, R_h, of the oligomer takes up to 2 days to reach its equilibrium value. Remarkably, the QLS experiments show that the rate of R_h increase at pH 6.4 is essentially the same at different peptide concentrations (Figures 4A and S5, Supporting Information). Therefore, the average aggregation

DOI: 10.1021/mp500519s
Mol. Pharmaceutics 2015, 12, 411−419

number of oligomers at any moment during the pH-induced transformation can be determined by SLS measurements (Figure 5A). The kinetics of aggregation number growth is

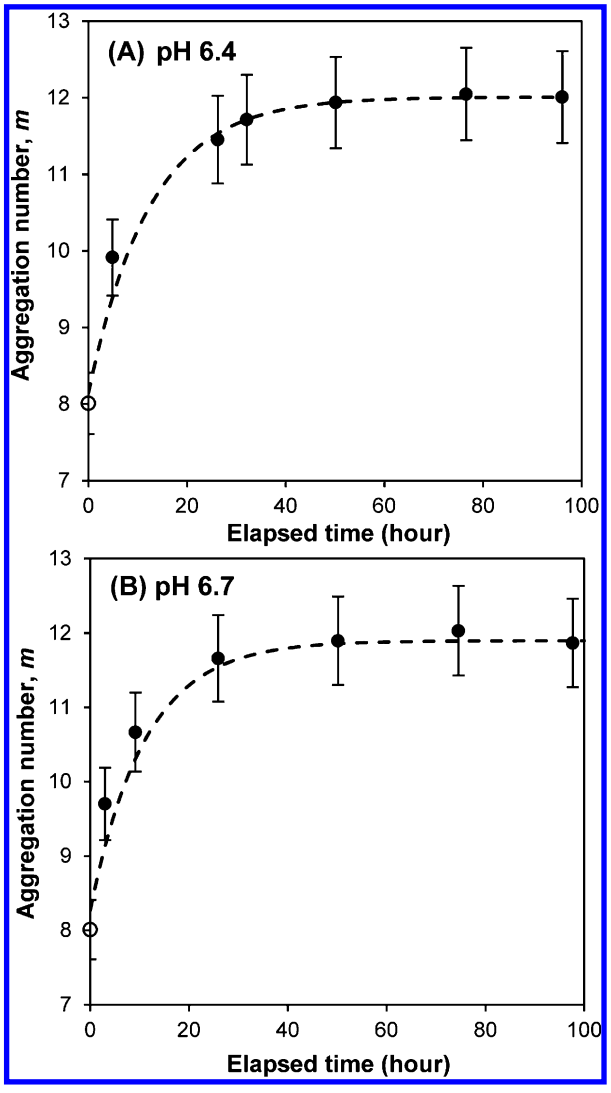

Figure 5. After the pH was lowered from 8.1 to (A) 6.4 and (B) 6.7, the average aggregation number of Liraglutide as a function of time was monitored by SLS at 22 °C. The open circles represent the aggregation number in the initial solutions at pH 8.1. The solid circles represent the average m in the solutions at pH 6.4 and pH 6.7. The dashed curves are the fits of the data with first order rate law as described in the discussion section.

consistent with that of the hydrodynamic radius growth. A similar kinetic profile of oligomer transformation has been observed at pH 6.7 (Figures 4B and 5B). The results of both QLS and SLS experiments (Figures 4 and 5) suggest an exponential kinetics of the oligomer transformation. The rate of this transformation appears to be similar at two different pHs.

The transformation of Liraglutide oligomer is reversible. Figure 6 shows the reverse oligomer transformation initiated by increasing pH back to 8.1 after incubation of the sample at pH 6.4 and 22 °C for 5 days. The size of oligomer decreased upon increasing pH and reached the equilibrium value at pH 8.1 within about 5 h. The reversibility of the oligomer transformation indicates that this transformation is caused solely by

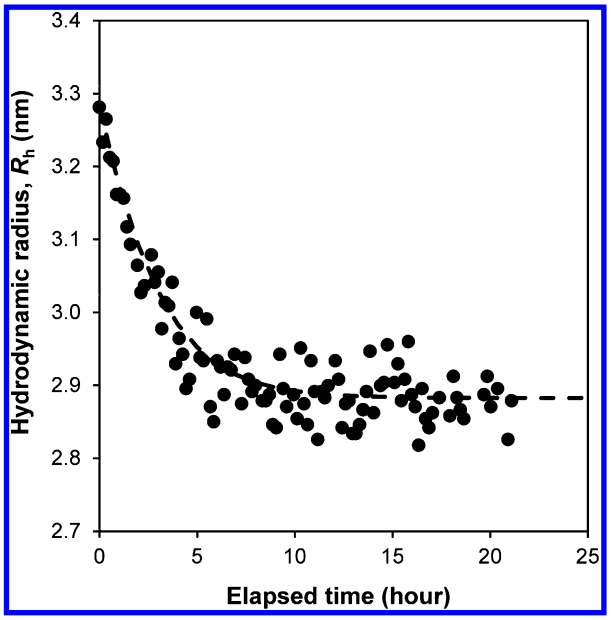

Figure 6. Decrease of hydrodynamic radius, R_h, during the reverse oligomer transformation in a 4 mg/mL Liraglutide solution monitored by QLS at 22 °C. The solution was incubated at pH 6.4 and 22 °C for 117 h before increasing pH. To initiate the reverse transformation, the pH was increased to pH 8.2.

protonation of the peptide and does not involve any irreversible pH-induced degradation.

pH-Induced Structural Changes of Liraglutide. The peptide structure in the Liraglutide oligomers changes during the pH-induced oligomer transformation. The secondary structure of Liraglutide was characterized using CD spectrometry. At pH above 6.9, the far-UV CD spectrum of Liraglutide is independent of pH (Figure 7) and remains unchanged for at least 10 days (Figure S6, Supporting Information). The spectrum has two minima at 208 and 222 nm indicating the presence of α helix elements in the structure. This result is consistent with the typical structure of the glucagon-like peptide family, which consists of α helix and random coil

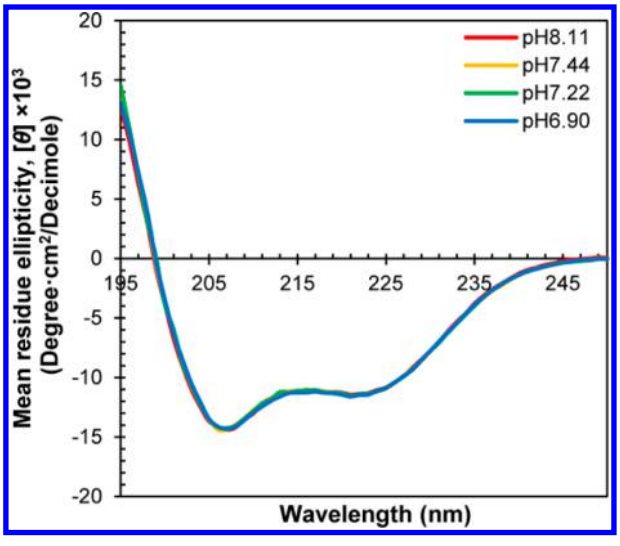

Figure 7. Far-UV CD spectra of Liraglutide at several pHs above 6.90 and 22 °C.

DOI: 10.1021/mp500519s
Mol. Pharmaceutics 2015, 12, 411−419

components (e.g., the structures of GLP peptides in Protein Data Bank:pdb 1gcn, 1d0r, 3iol, 2l64, and 2m5p).

When pH was lowered below 6.90, the secondary structure of Liraglutide within the oligomer changed significantly over time (Figure 8A for pH 6.40 and Figure 8B for pH 6.70). These

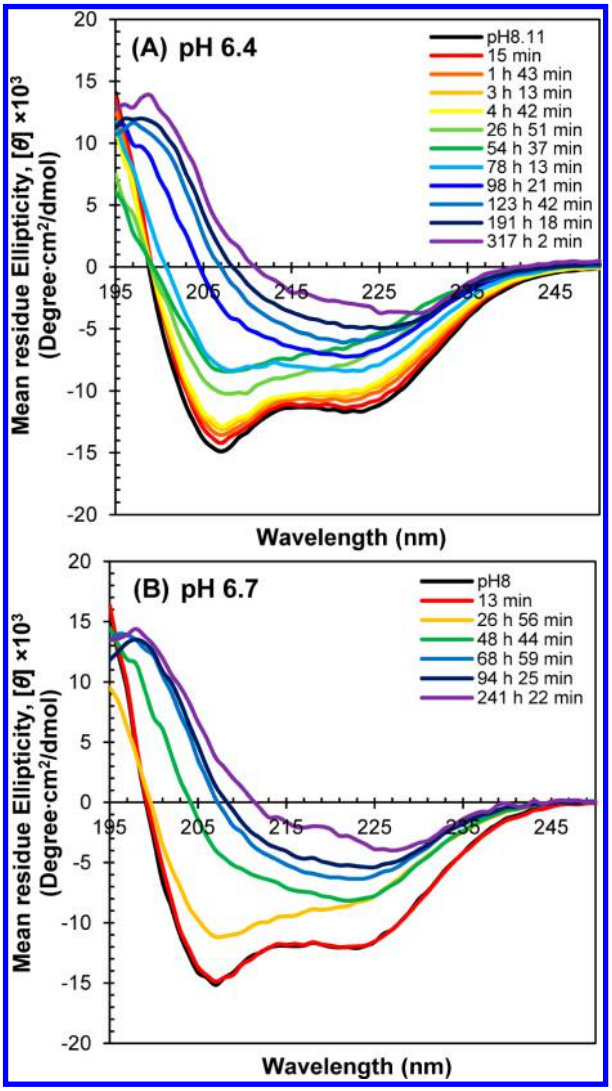

Figure 8. Evolution of the CD spectra of Liraglutide over time at 22 °C, after pH was lowered from 8.11 to (A) 6.40 and (B) 6.70.

figures show that the α helix components gradually convert into other structural elements. The structural change in the first 2 days concurs with the change of oligomer size monitored by the light scattering experiments. After these 2 days, the peptide structure continues changing slowly for up to 10 days, while the size of the oligomer remains constant (Figure S7, Supporting Information). Similar to the change in the size of the oligomer (Figure 6), the structural change is completely reversible when pH is increased back to 8.1 during the transformation (Figures S8 and S9, Supporting Information).

DISCUSSION

Liraglutide is an amphiphile that consists of a mainly hydrophilic peptide and a hydrophobic fatty acid chain. In general, peptide amphiphiles are known to form assemblies that are conceptually analogous to micelles of small molecule surfactants.[15] Similar to micelles, the oligomer is held together by noncovalent interactions and should be in equilibrium with the monomer. The monomer concentration, analogous to the critical micelle concentration (CMC), of Liraglutide is reported to be as low as ~1 μM (~4 μg/mL).[21] Therefore, under our experimental conditions, Liraglutide exists predominantly in the form of oligomers.

We observed a sharp transition in both size and structure of Liraglutide oligomers at pH around 6.9. Generally, pH determines the protonation states of amino acid residues in peptides and thereby affects their solution stability, molecular structure, and biological function. Protonation of Liraglutide at pH below 6.9 alters both inter- and intrapeptide interactions and leads to subsequent changes in the oligomer size and the peptide structure observed in this work. In Liraglutide, the ionic functional group having pK_a closest to 6.9 is the side chain of the N-terminal histidine (pK_a = 6.04 estimated by that in free amino acids; Figure S10, Supporting Information). Thus, the most significant change of protonation below pH 6.9 is likely to occur on the histidine. In fact, the presence of histidine is known to increase the pH sensitivity of the structures and functions of other peptides at pH near 7.[26−28]

A striking feature of the pH-induced oligomer transformation of Liraglutide is its slow kinetics. When pH is lowered from that above 6.9 to either 6.4 or 6.7, Liraglutide oligomer changes from 8mer into 12mer. In this transformation, 8mers have to at least partially dissociate into monomers and reassemble into 12mers. Dissociation of 8mers is caused by monomer desorption from the oligomers, and thus, the 8mer dissociation rate reflects the effective monomer desorption rate. Our kinetic CD measurements in Figure 8 show that, within the first 5 h after lowering pH, the peptide structure is similar to the initial structure. This result suggests that a significant amount of original 8mers remains in the solution in the early stage of the pH-induced transformation. Therefore, we can make the assumption that monomer desorption from the 8mers is the rate-limiting step for the transformation of Liraglutide from 8mer to 12mer.

With this assumption, we analyze the kinetics of the pH-induced transformation measured by QLS and SLS experiments. We denote the mass concentrations of 8mer and 12mer, respectively, as c_1 and c_2, and the total Liraglutide concentration $c_0 = c_1 + c_2$. Here, we assume that the mass concentration of monomer is negligible. After initiation of the oligomer transformation by lowering pH, c_1 decreases and c_2 increases. The reduction in 8mer concentration should follow the first order rate law $dc_1/dt = -k_1^- c_1$, where k_1^- is the rate constant of monomer desorption from the 8mers. Then, at a time t after lowering pH, the oligomer concentrations are $c_1 = c_0 e^{-k_1^- t}$ and $c_2 = c_0(1 - e^{-k_1^- t})$. Using these expressions, we can fit our kinetic data of QLS and SLS experiments and determine the rate constant k_1^- as described below.

In QLS measurements, the hydrodynamic radius is derived from the diffusion coefficient using the Stokes−Einstein equation: $R_h(t) = kT/6\pi\eta D(t)$, where k is the Boltzmann constant, T is the solution temperature, and η is the solvent viscosity. In our case, the apparent diffusion coefficient is the z-average of diffusion coefficients of both oligomers: $D(t) = (c_1 m_1 D_1 + c_2 m_2 D_2)/(c_1 m_1 + c_2 m_2)$ where $m_1 = 8.0 \pm 0.4$ and $m_2 = 12.0 \pm 0.6$ are, respectively, the aggregation numbers of the 8mer and the 12mer measured in the SLS experiments. D_1 and D_2 are their diffusion coefficients measured in QLS experi-

DOI: 10.1021/mp500519s
Mol. Pharmaceutics 2015, 12, 411−419

ments. Then, the apparent hydrodynamic radius as a function of time can be expressed as $R_h(t) = kT(c_1m_1 + c_2m_2)/6\pi\eta(c_1m_1D_1 + c_2m_2D_2)$. We have used this equation with the expressions of c_1 and c_2 given in the previous paragraph to fit the experimentally measured $R_h(t)$ at pH 6.4 and 6.7 (Figure 4) and obtained the dissociation rate constants for the 8mer: $k_1^- = 0.07 \pm 0.02\ h^{-1}$ at pH 6.4 and $k_1^- = 0.06 \pm 0.02\ h^{-1}$ at pH 6.7. Note that, within the experimental error, the rate constants are the same at pH 6.4 and pH 6.7.

In SLS measurements, the apparent aggregation number is the weight-average of that of 8mer and 12mer: $m(t) = (c_1m_1 + c_2m_2)/c_0$. In Figure 5, we show that our SLS data is consistent with the theoretical curve calculated using the rate constant $k_1^- = 0.07\ h^{-1}$.

The monomer desorption model of the pH-induced oligomer transformation of Liraglutide is summarized in Figure 9. In this model, the oligomers are in equilibrium with

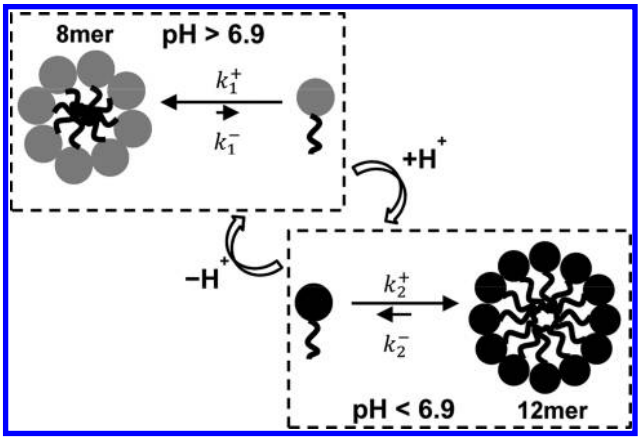

Figure 9. Scheme of the monomer desorption model for the pH-induced oligomer transformation of Liraglutide. k_1^+ and k_1^- are, respectively, the monomer adsorption and desorption rate constants for 8mer. k_2^+ and k_2^- are, respectively, the monomer adsorption and desorption rate constants for 12mer. The dark circles represent the protonated peptide at low pH.

monomer, and monomer constantly escapes from or associates with the oligomers. In Figure 9, we denote the monomer adsorption and desorption rate constants, respectively, as k_1^+ and k_1^- for 8mer and k_2^+ and k_2^- for 12mer.

At pH above 6.9, our experimental results show that the 8mer is the dominant oligomer and that the monomer concentration is very low. Thus, $k_1^+ \gg k_1^-$. When pH is lowered to a value below 6.9, the protonation state of the peptide is changed, and the 12mer becomes more stable than the 8mer. At a result, the 8mers gradually dissociate and the 12mers are formed.

Importantly, the monomer desorption rate constant is the same at different pHs. One can hypothesize that the monomer desorption rate is insensitive to the charges on the peptides and mainly dependents on the entropic advantage of packing the hydrophobic lipid chain inside the oligomer. Thus, we can expect that the value of k_1^- determined in our experiment is also a good approximation of the monomer desorption rate constant in the whole range of pH values around physiological pH. This rate constant, $k_1^- = 0.07\ h^{-1}$, corresponds to a 10 h half-life of monomer desorption from the 8mer. With a pH-insensitive k_1^-, dissociation of the original 8mers at low pH suggests a decrease in the adsorption rate constant k_1^+.

Similarly, we can analyze the kinetics of the reverse transformation from 12mer to 8mer when pH is raised from 6.4 to 8.1. By fitting the QLS kinetics data for the reverse transformation (Figure 6), we have obtained the rate constant $k_2^- = 0.4 \pm 0.1\ h^{-1}$, which corresponds to a 2 h half-life of monomer desorption from the 12mer. Remarkably, the monomer desorption rate constant of the Liraglutide 12mer is about five times faster than that of the 8mer. In other words, the 12mer formed at low pH is a much less stable assembly than the original 8mer at high pH.

To further our understanding of the structural changes during the pH-induced transformation of Liraglutide oligomer, the time-dependent CD spectra (Figure 8) were decomposed using CDPro software package.[29] The changes of the characteristic structural elements during the transformation are summarized in Figure 10. Within the first 2 days, the kinetics of the structural change concurs with the change of oligomer size observed by QLS and SLS. The structural change continues for up to 10 days after the size of oligomer reaches equilibrium. This process can be understood as a slow

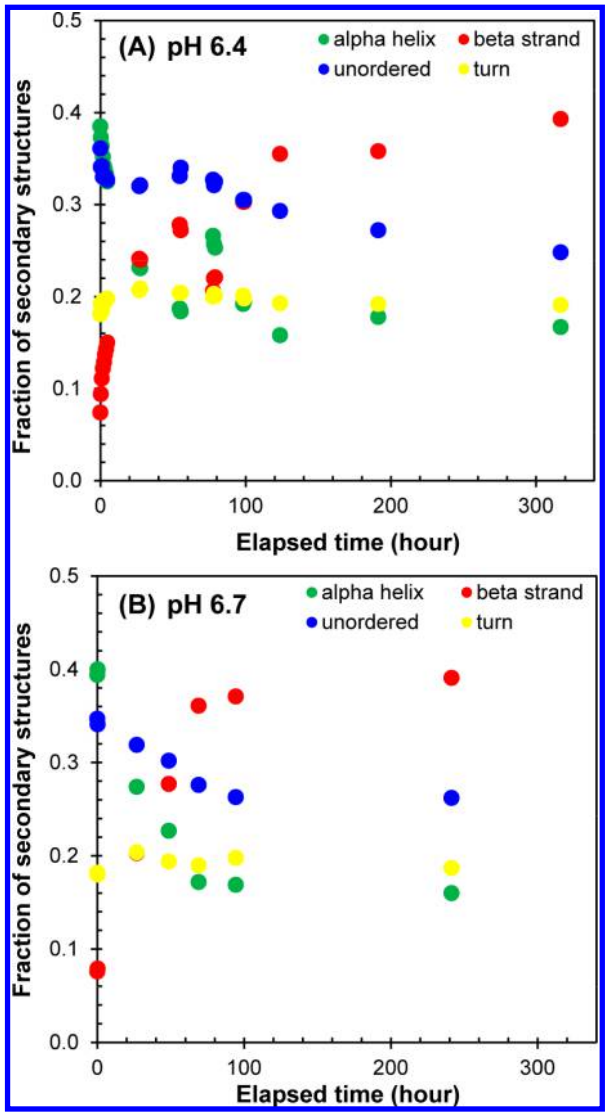

Figure 10. Changes of structural elements at (A) pH 6.4 and (B) pH 6.7 over time at 22 °C. The solid points are the results of decomposition of CD spectra in Figure 8 using CDPro CONTINLL.

DOI: 10.1021/mp500519s
Mol. Pharmaceutics 2015, 12, 411−419

maturation of the newly formed 12mer to its thermodynamically stable structure. The kinetic CD data suggests that the two-stage kinetic pattern and its time scale are very similar at the two different pHs. This result supports the suggestion that the monomer desorption is the rate limiting step for the transformation. Indeed, if the other processes involving interactions of protonated amino acid residues were involved, one would expect a pH-depending kinetics of the transformation.

The rate of monomer desorption from micelle-like assemblies is a fundamental property of peptide amphiphiles, which affects various aspects of the pharmacokinetics of peptide pharmaceuticals.[15−18] For the soluble peptides, the monomer desorption rate is mainly controlled by the size and number of the hydrophobic lipid chains in the assemblies.[15] In previous studies, the monomer desorption rate was measured under different conditions using the fluorescence quenching method.[15−17] The desorption rate constant, ranging from seconds to hundreds of hours, depends on both the properties of peptide amphiphiles and the solution environments such as temperature, salt, and other excipients in the solution.[16,17] In this work, we have demonstrated that the monomer desorption rate of Liraglutide at various solution conditions can be measured through monitoring the kinetics of the pH-induced oligomer transformations using QLS. As it does not require preparation of fluorophore-tagged peptides, this approach provides a useful tool to evaluate the monomer desorption rate of Liraglutide as well as similar peptide amphiphiles that also exhibit slow pH-induced oligomer transformation.

■ CONCLUSION

In this work, we studied a pH-induced transformation of the micelle-like oligomer of Liraglutide. Liraglutide is a representative of incretin-like drugs, a group of peptides that draws significant interest from the pharmaceutical industry. These small peptides, like natural hormones, have a very short circulation lifetime in their naked form, and the lipidation is one common approach to improve their pharmacokinetic properties. In this work, we observed that, when pH is lowered below 6.9, the 8mer of Liraglutide slowly transforms into 12mer. During the transformation from 8mer to 12mer, the peptide gradually loses its α helix structural elements. This oligomer transformation is fully reversible upon increasing pH. The slow and pH-insensitive kinetics of this transformation suggests that the monomer desorption from the oligomer is the rate-limiting step of the transformation. The monomer desorption rate constant was determined by monitoring the kinetics of the oligomer transformation. The monomer desorption rate is an important factor that affects the pharmacokinetics of bioactive peptide amphiphiles. Our study on Liraglutide oligomerization sheds light on the solution behavior of lipidated peptides, in particular the GLP-1 agonists. In the future studies, it is important to investigate other lipidated incretin peptides to examine the universality of the pH-induced oligomer transformation. The results of these studies in conjunction with the pharmacokinetic data would be invaluable for developing lipidated incretin drugs.

■ ASSOCIATED CONTENT

Supporting Information

Sequence of Liraglutide and Figures S1−S10. This material is available free of charge via the Internet at http://pubs.acs.org.

■ AUTHOR INFORMATION

Corresponding Author

*Tel: 617-253-4828. Fax: 617-253-0359. E-mail: benedek@mit.edu.

Notes

The authors declare no competing financial interest.

■ ACKNOWLEDGMENTS

This work is supported by the Roche Postdoctoral Fellowship (RPF) Program. We thank the Biophysical Instrumentation Facility (BIF) at MIT for the use of the Wyatt light scattering instrument and the CD spectrometer. We thank Ms. Debby Pheasant at BIF for providing the technical support of the BIF instruments.

■ REFERENCES

(1) Craik, D. J.; Fairlie, D. P.; Liras, S.; Price, D. The future of peptide-based drugs. *Chem. Biol. Drug Des.* **2013**, *81*, 136−147.

(2) Kaspar, A. A.; Reichert, J. M. Future directions for peptide therapeutics development. *Drug Discovery Today* **2013**, *18*, 807−817.

(3) Crunkhorn, S. Anticancer drugs: Stapled peptide reactivates p53. *Nat. Rev. Drug Discovery* **2013**, *12*, 741.

(4) Meier, J. J. GLP-1 receptor agonists for individualized treatment of type 2 diabetes mellitus. *Nat. Rev. Endocrinol.* **2012**, *8*, 728−742.

(5) Drucker, D. J.; Nauck, M. A. The incretin system: glucagon-like peptide-1 receptor agonists and dipeptidyl peptidase-4 inhibitors in type 2 diabetes. *Lancet* **2006**, *368*, 1696−1705.

(6) Holst, J. J. The physiology of glucagon-like peptide 1. *Physiol. Rev.* **2007**, *87*, 1409−1439.

(7) Willard, F. S.; Sloop, K. W. Physiology and emerging biochemistry of the glucagon-like peptide-1 receptor. *Exp. Diabetes Res.* **2012**, *2012*, 470851.

(8) Knudsen, L. B.; Nielsen, P. F.; Huusfeldt, P. O.; Johansen, N. L.; Madsen, K.; Pedersen, F. Z.; Thogersen, H.; Wilken, M.; Agerso, H. Potent derivatives of glucagon-like peptide-1 with pharmacokinetic properties suitable for once daily administration. *J. Med. Chem.* **2000**, *43*, 1664−1669.

(9) Clodfelter, D.; Pekar, A.; Rebhun, D.; Destrampe, K.; Havel, H.; Myers, S.; Brader, M. Effects of non-covalent self-association on the subcutaneous absorption of a therapeutic peptide. *Pharm. Res.* **1998**, *15*, 254−262.

(10) Zhang, L.; Bulaj, G. Converting peptides into drug leads by lipidation. *Curr. Med. Chem.* **2012**, *19*, 1602−1618.

(11) Havelund, S.; Plum, A.; Ribel, U.; Jonassen, I.; Vølund, A.; Markussen, J.; Kurtzhals, P. The mechanism of protraction of insulin detemir, a long-acting, acylated analog of human insulin. *Pharm. Res.* **2004**, *21*, 1498−1504.

(12) Li, Y.; Shao, M.; Zheng, X.; Kong, W.; Zhang, J.; Gong, M. Self-assembling peptides improve the stability of glucagon-like peptide-1 by forming a stable and sustained complex. *Mol. Pharmaceutics* **2013**, *10*, 3356−3365.

(13) Khan, S.; Sur, S.; Newcomb, C. J.; Appelt, E. A.; Stupp, S. I. Self-assembling glucagon-like peptide 1-mimetic peptide amphiphiles for enhanced activity and proliferation of insulin-secreting cells. *Acta Biomater.* **2012**, *8*, 1685−1692.

(14) Ward, B. P.; Ottaway, N. L.; Perez-Tilve, D.; Ma, D.; Gelfanov, V. M.; Tschop, M. H.; Dimarchi, R. D. Peptide lipidation stabilizes structure to enhance biological function. *Mol. metab.* **2013**, *2*, 468−479.

(15) Trent, A.; Marullo, R.; Lin, B.; Black, M.; Tirrell, M. Structural properties of soluble peptide amphiphile micelles. *Soft Matter* **2011**, *7*, 9572−9582.

(16) Missirlis, D.; Krogstad, D. V.; Tirrell, M. Internalization of p53(14−29) peptide amphiphiles and subsequent endosomal disruption results in SJSA-1 cell death. *Mol. Pharmaceutics* **2010**, *7*, 2173−2184.

DOI: 10.1021/mp500519s
Mol. Pharmaceutics 2015, 12, 411−419

(17) Kastantin, M.; Missirlis, D.; Black, M.; Ananthanarayanan, B.; Peters, D.; Tirrell, M. Thermodynamic and kinetic stability of DSPE-PEG(2000) micelles in the presence of bovine serum albumin. *J. Phys. Chem. B* **2010**, *114*, 12632−12640.
(18) Dong, H.; Dube, N.; Shu, J. Y.; Seo, J. W.; Mahakian, L. M.; Ferrara, K. W.; Xu, T. Long-circulating 15 nm micelles based on amphiphilic 3-helix peptide-PEG conjugates. *ACS Nano* **2012**, *6*, 5320−5329.
(19) Yu, Y. C.; Pakalns, T.; Dori, Y.; McCarthy, J. B.; Tirrell, M.; Fields, G. B. Construction of biologically active protein molecular architecture using self-assembling peptide-amphiphiles. *Methods Enzymol.* **1997**, *289*, 571−587.
(20) Yu, Y.-C.; Berndt, P.; Tirrell, M.; Fields, G. B. Self-assembling amphiphiles for construction of protein molecular architecture. *J. Am. Chem. Soc.* **1996**, *118*, 12515−12520.
(21) Steensgaard, D. B.; Thomsen, J. K.; Olsen, H. B.; Knudsen, L. B. The molecular basis for the delayed absorption of the once-daily human GLP-1 analogue, liraglutide. (Abstract 552-P). *Diabetes* **2008**, *57*, A164.
(22) Nauck, M. A. Liraglutide, a once-daily human GLP-1 analogue. *Br. J. Diabetes Vasc. Dis.* **2008**, *8*, S26−S33.
(23) Pike, E. R.; Pomeroy, W. R. M.; Vaughan, J. M. Measurement of Rayleigh ratio for several pure liquids using a laser and monitored photon counting. *J. Chem. Phys.* **1975**, *62*, 3188−3192.
(24) Wang, Y.; Lomakin, A.; McManus, J. J.; Ogun, O.; Benedek, G. B. Phase behavior of mixtures of human lens proteins Gamma D and Beta B1. *Proc. Natl. Acad. Sci. U.S.A.* **2010**, *107*, 13282−13287.
(25) Slifkin, M. A.; Ali, S. M. Measurements of protonation reaction kinetics of histidine using a chemical relaxation technique. *J. Mol. Liq.* **1984**, *28*, 165−174.
(26) Armstrong, K. M.; Baldwin, R. L. Charged histidine affects alpha-helix stability at all positions in the helix by interacting with the backbone charges. *Proc. Natl. Acad. Sci. U.S.A.* **1993**, *90*, 11337−11340.
(27) Callahan, D. J.; Liu, W.; Li, X.; Dreher, M. R.; Hassouneh, W.; Kim, M.; Marszalek, P.; Chilkoti, A. Triple stimulus-responsive polypeptide nanoparticles that enhance intratumoral spatial distribution. *Nano Lett.* **2012**, *12*, 2165−2170.
(28) Tu, Z.; Volk, M.; Shah, K.; Clerkin, K.; Liang, J. F. Constructing bioactive peptides with pH-dependent activities. *Peptides* **2009**, *30*, 1523−1528.
(29) Greenfield, N. J. Using circular dichroism spectra to estimate protein secondary structure. *Nat. Protoc.* **2006**, *1*, 2876−2890.

DOI: 10.1021/mp500519s
Mol. Pharmaceutics 2015, 12, 411−419